



# Case study of Block 1, Highland Towers Condominium collapsed in Taman Hillview, Ulu Klang, Selangor, Malaysia on 11th December 1993

Solahuddin Bin Azuwa<sup>\*</sup>, Fadzil Bin Mat Yahaya

Faculty of Civil Engineering Technology, Level 1, Chancellery Building, Universiti Malaysia Pahang Al-Sultan Abdullah, Lebuhr Persiaran Tun Khalil Yaakob, 26300 Kuantan, Pahang Darul Makmur, Malaysia

## ARTICLE INFO

**Keywords:**  
Case study  
Building collapse  
Landslide  
Highland Towers condominium  
Selangor  
Malaysia

## ABSTRACT

Landslide has become the primary focus in slope engineering as the case increases. Most landslides are resulted from an unknown confluence, and most occur on slopes created by humanity. Highland Towers were built between 1976 and 1979, and its occupants were primarily first and middle-class people. There is a steep hill behind the three blocks. The main draws here are the natural scenery and panoramic vista of Kuala Lumpur. This case study investigates what factors led to Block 1, Highland Towers condominium's collapse on 11th December 1993 at 1.35 p.m. using reliability analysis approaches and human fault impact factors. The Block 1 collapse is caused by an unstable pile foundation. The engineers incorrectly estimated the horizontal load design, causing surcharge loads to be created by the downhill forward movement when the rotating retrogressive slide happens. However, several precautions may be taken to protect the building structures from landslide. It is common knowledge that structural reliability analysis yields failure probabilities that are not considered for human faults. Inadequate drainage, collapse of retaining wall, and rail piling foundation are all plausible explanations for this landslide initiation. Thus, combining structural and human reliability analysis are recommended to mitigate landslide, including slope hazards.

## 1. Introduction

The landslide term refers to the downward movement of a large quantity of rock, rubble, or dirt. A landslide is a form of mass wasting, defined as a downslope movement of soil and rock under gravity. Moreover, a landslip can refer to any of five different types of slope movements, like falling, toppling, sliding, spreading, or flowing. Each is further classified as either bedrock, residue, or earth. Common landslip types include debris flow, mudflow, mudslide, and rock fall. Several factors contribute to almost all landslides. Movement occurs when the downward gravity force surpasses the earth's component strength, making up a slope. Factors that amplify downslope forces diminish the strength produced. Rainfall, snowmelt, changes in water level, stream erosion, changes to groundwater, earthquakes, volcanic activity, disturbance by human activities, and the like can trigger a slope landslide. Several different things, including earthquake activity, cause underwater landslide. A tsunami can be caused by a landslide occurring under the ocean, which can devastate coastal regions.

Despite the relatively flat topography, slope failure and landslide are common in Malaysia. Mountains and hills make up less than 25% of the

land. Rain is one of the factors that cause the slope to collapse. However, the researcher has found that this is not the only explanation by studying several related landslide cases. Most slope landslides occur that are created by humans on the earth. This landslide is primarily due to human errors and mistakes such as poor planning, shoddy artistry, or neglectful upkeep [1]. According to a Malaysian government body, Public Work Department, 90% of landslides are associated with constructed slopes [2,3]. Gue and Tan (2017) [4] conclude that raw input data is a factor in the prevalence of landslide coupled with worst design, incompetence, and casualness. This case study highlights and discusses five crucial things: (1) details and chronologies of the collapse, (2) discussion about the causes of the collapse, (3) methods that shall be taken to prevent landslide, (4) conclusion, and (5) recommendation. There are three main methods to prevent landslide from occurring discussed in this article: (1) retaining wall construction, (2) rock bolts installation, and (3) vegetative plantation.

## 2. Literature review on landslide

Three landslide inventories and universal frequency area statistics

<sup>\*</sup> Corresponding author.

E-mail address: [solahuddin.08@yahoo.com](mailto:solahuddin.08@yahoo.com) (S. Bin Azuwa).

have been examined and compared by Reis & Gins (2017) [5]. They evaluate the significance of landslip analysis based on the completeness and resolution of landslip inventory maps. The number of landslip cases increased exponentially with the landslip area and then decreased as a power law function until a certain threshold was reached. Systematic surveys using aerial photo interpretation and GIS databases allowed the creation of landslip inventory map Wang et al. (2023) [6]. The landslide classification format was used to identify the landslide types Khodabakhsh et al. (2018) [7]. Maps of landslip inventories were prepared, identified and compared to other regions in Italy He & Wang (2018) [8]. They compiled geomorphological landslip maps and multi-temporal landslip inventories to establish a good connection between them. Moreover, the findings also indicated that the landslide inventory maps were handy in predicting similar incidents. The precision of landslip analysis was affected by the thoroughness and accuracy of the landslip inventory. The information on landslip maps, photos, and archives was used to generate landslip inventory maps for various trigger events Ren & Ni (2020) [9]. In order to analyse the temporal and magnitude probabilities, these maps should depict landslip patterns and types of triggering events with a spectrum of return times. Behmanesh & Rahimi (2012) [10] created semi-automatic image analysis methods using precise, high-resolution satellite data and DTM to create landslip inventories. The study's most significant contribution and novelty is the method used to choose and pick up the best diagnostic characteristics for landslip and apply them to all-encompassing characterisation of various landslip types. The first idea was from Gundu & Simon (2021) [11], which focused on landslip detection in an object-oriented setting.

### 3. Case study

This section explains and discusses the case study in detail, including the tragedy sequences and chronologies of the collapse of Block 1, Highland Towers condominium. The Malaysian area of Ulu Klang is prone to landslide. Specifically, the coordinates ( $4^{\circ}10'26''-4^{\circ}14'46''$  East,  $102^{\circ}5'14''-102^{\circ}48'52''$  North) denote the location of Kuala Lumpur, the capital of Malaysia. Landslide and mudflow are two primary issues of urbanisation in this area. Several tragic landslip caused by heavy rain occurred in the Ulu Klang region. Since 1980, 30 large landslip incidents have occurred. One of the worst tragedies was that 48 people died when a Highland Towers Condominium at Taman Hillview, Ulu Klang, Selangor, Malaysia, collapsed after a few days of rain in 1993. The Malaysian Meteorology Association (MMA) reports that the average temperature in Ulu Klang is between 28 and 30 °C, while the average relative humidity is between 70% and 75%, which is critical. The Malaysian yearly mean temperature is around 26 °C, while the Malaysian sweltering months are March, April and May. June, July, and August are the driest months in Malaysia. Fig. 1 shows the location map of Ulu Klang.

The Highland Towers condominium has three building Blocks, each with 12 stories. Between 1974 and 1990, it was constructed in several stages. Blocks 1, 2 and 3 were entirely built in 1975, 1985, and 1990. Block 1 is located in the southernmost region. Block 2 is located northwest of Block 1, while Block 3 is situated west of Block 2. The Highland Towers were residences by upper and middle-class families, including local Malaysian people and foreigners. On 11th December



Fig. 1. Location map of Ulu Klang, Selangor, Malaysia.



1993, at 1.40 p.m., Block 1 collapsed. This is the earliest one of Malaysia’s worst tragedies happened in Malaysian history when a building with many units on multiple floors collapsed. Forty-eight people died. Blocks 2 and 3 residents were not allowed to enter their houses by the authorities called Majlis Perbandaran Ampang Jaya (MPAJ) and Polis Diraja Malaysia (PDRM) after the fall of Block 1 to prevent the catastrophe repetition. They were evacuated to a safer place for safety protection. A very steep hill is laid behind the three Blocks. The slope is crossed by a creek from land to hill. In 1980 and early 1990, the Highland Towers condominium earned a bad reputation in the affluent society. Figs. 2 and 3, Table 1 show the tragedy sequences and chronologies of the collapse of Block 1, Highland Towers condominium [4].

#### 4. Discussion of the causes of the collapse

Ten consecutive days of non-stop heavy rain caused the diversion pipes to fail, leading to a massive landslide that ultimately led to the collapse of Block 1. Inadequate soil testing contributes to the landslide disaster. Undermining occurs as a result of site exploration. The collapse of the building structure was exacerbated by a landslide caused by the collapse of retaining walls during the ten days of heavy rain. Disturbances to the slope’s inherent stability lead to landslide. They can occur before, during, or after natural disasters like floods, earthquakes, or volcanic eruptions. Rapid groundwater accumulation can cause mudslide, a rush of water-soaked rock, soil, and debris. Mudslide is often begun on steep slopes and triggered by weather or geological factors. Areas where wildfires or human acts devastate vegetation on ground and hillsides, causing landslide to occur easily and quickly during and after heavy rains. Moreover, improper soil bearing tests, failure to identify the

lousy condition during a pre-construction site visit in pre-design phase, and inadequate retaining wall design are the landslide factors [12–16]. Furthermore, the heavy rain triggers a retrogressive landslide behind Block 1, leading to rail piling foundation instability, which cannot withstand the lateral stress. The surface runoff and infiltration rates increase, causing the slope materials to lose, followed by the inclination of the landslide chain reaction [17,18]. Besides that, the drainage flow system is also poor and lacks maintenance. In addition to the numerous previous landslide that have occurred nearby, the landslide at Highland Towers is being studied in detail since it causes substantial compensatory and non-compensatory building damages. Fig. 4 demonstrates block 1’s cross-section, including side, front and plan views [18], while Fig. 5 illustrates retrogressive landslide.

The landslide happened because of poor planning execution during the condominium construction. All the Highland Towers Blocks were built using cut-and-fill techniques. This building method uses a retaining wall to keep the terrain in place. Three separate instances of lateral pressure from underground land movement collapse the retaining wall behind Block 1. Fig. 6 shows the retrogressive slips when the landfill is improperly compacted in the development area. The construction and development activities at a high level cause the debris to flow and slide, impacting the low level of Block 1, as delineated in Figs. 7 and 8. A new platform level is required to redirect the water flow from the old path in the Highland Towers project. The artificial water stream will continue to run along its established way indefinitely. Besides that, the retaining wall produces a tremendous strain, which might eventually lead to its collapse. If the building is on a slope, it should be checked whether it is located near the land or not [19,20]. Any nearby development or building will affect the ground stability. Thus, this must be considered while deciding the best design strategy. Furthermore, the Highland

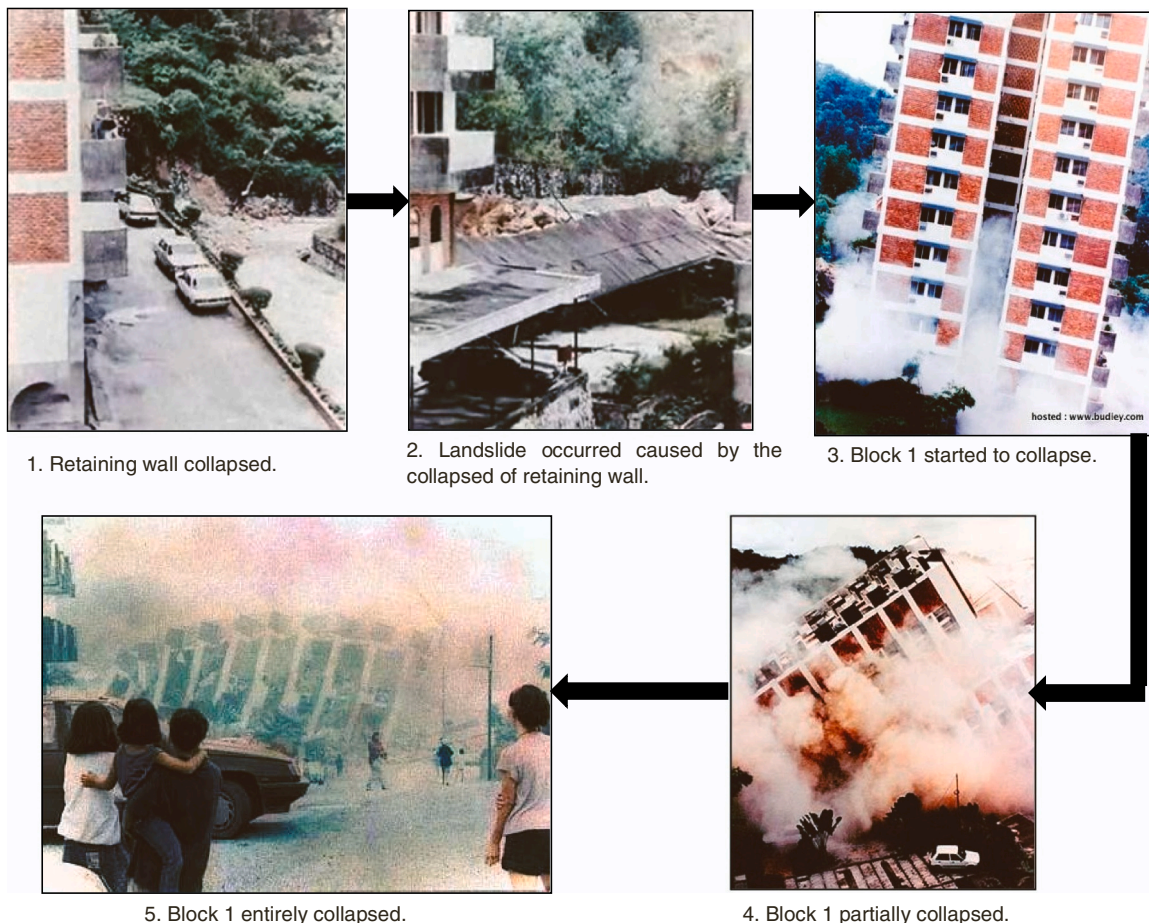


Fig. 2. Tragedy sequences .



Fig. 3. Blocks 2 and 3, which are firmly standing until now.

Towers condominium construction works at the hillside failed, followed by rubble crashing. The landslide causes retaining wall failure, which slides downward. The landslide is not expected to occur because of improper land maintenance. This improperly preserved land causes several effects, such as water flow impedes, water pounding, and soil stability reduction [21]. The Highland Tower development has this problem as the terrain becomes unstable from water pounding due to a lack of maintenance activities.

The pile foundation of Highland Towers is unstable, which leads to the building's collapse. When the rotating retrogressive slide happens, the downhill forward movement creates a surcharge load over the foundation since the engineer did not correctly estimate the horizontal load design. Moreover, it collapses because its foundation cannot withstand horizontal loads due to landslide. Since landslide is becoming more common, slope engineering is currently a top priority. The artificial slope is considered the leading cause of landslide failures. Thus, this issue shall be addressed immediately. This landslide occurs because of bad city planning, shoddy quality, and lack of technical knowledge. According to one assessment from a specific industry in Malaysia, 90% of 50 big landslide in a country can be traced back to the slopes created by humanity [22,23]. The necessity to methodologically address the uncertainty caused by human variables is still not widely acknowledged. Some experts agree that the tensions ruling with soil parameters and the chosen models are analogous to the delays in building construction projects. The Malaysian authorities also acknowledged the significance of human uncertainty factors. In the simplest form, human reliability analysis determines how much attention should be paid to various sources of uncertainty arising from human activities that cause landslide. When discussing building designs, the influence of human uncertainty under the label of the humanity factor is also recorded [24–26]. The human factor term describes a physical or cognitive characteristic of individual or societal behaviour that seems unique to humans and affects the technology operation system and human environment. Subsequently, human factors are depicted as the primary cause of the uncertainty increases. These human factors are challenging to consider during the building designs, which can cause stress on the reliability and safety of a building. Errors in the design and construction of a product or system might occur when the relevant information for failure avoidance is unavailable, unused, or wrongly used in the design applied in a component system [27–29].

## 5. Methods to prevent landslide

There are several methods to prevent landslide, such as retaining wall construction, rock bolt installation and vegetative plantation. There are two types of retaining walls that shall be built, which are gravity and cantilever retaining walls, while four types of rock bolts shall be

installed: (1) wedge blocks at wall, (2) arching bolting, (3) tieback bolting, and (4) suspension bolting. For vegetative plantations, fifteen types of green plants shall be planted on the ground. All these methods are essential in preventing landslide from occurring.

### 5.1. Retaining wall construction

#### 5.1.1. Gravity

When earth or other material substances are piled up behind a wall, the wall is considered a gravity retaining wall [30–32]. The purpose of gravity retaining wall is to prevent potential landslide by detaining the soil's lateral force load [33–35]. Besides that, it is also a crucial structural component of highways and other environmental constructions when constructed on contoured soils or soils with varying elevations [36,37]. The size and location of the area where lateral soil pressure acts must be fully and carefully investigated before constructing a gravity retaining wall or any other retaining wall. The gravity retaining wall design must be correctly calculated to save it from hazards and disasters. In order to properly plan the gravity retaining wall construction, it is necessary to identify several factors at the site, like soil type, sliding angle, and weight of soil volume [38]. Several studies recommend that the gravity retaining wall be designed to withstand slope earthquakes [39,40]. Fig. 9 shows the gravity retaining wall.

### 5.2. Dimension of gravity retaining wall

The proposed length of the gravity retaining wall used in this case study is 4–4.5 km. The value details are delineated in Table 2, while the gravity retaining wall dimension is depicted in Fig. 10.

### 5.3. Stability

Active soil coefficient,  $A = 0.48$

$$\text{Horizontal force, } B = \frac{1}{2} \times R \times C^2 \times A = \frac{1}{2} \times 1.57 \times 7.36^2 \times 0.48 = 20.41 \text{ tonnes} \quad (1)$$

$$\text{Arm turning point, } D = \frac{1}{3} \times 7.36 = 2.45 \text{ m} \quad (2)$$

$$E = B \times D = 20.41 \times 2.45 = 50 \text{ tonnes.m} \quad (3)$$

The calculation results produce horizontal force (B) = 20.41 tonnes and moment (E) = 50 tonnes.m.

From Table 3,  $\Sigma F = 39.19$  tonnes with  $\Sigma H = 123.52$  tonnes.m, and  $I_1 = 66.22$  tonnes.m

**Table 1**  
Chronologies with year occurred.

Year	Chronologies
1978	The southernmost tower, known as Block 1, was built.
1980	Block 2 was slightly taller than the other two blocks and situated northwest of Block 1.
1982	Block 3 was built between the northwest and west of Blocks 1 and 2, respectively.
1990	New homes were being built on the ridge behind all blocks as a part of the building construction project. The hill was stripped of its trees and other plants, leaving the soil vulnerable to erosion and triggering a landslide to occur.
1992	<b>December:</b> The ruptured pipes produced the flood, causing the water to pour down the hill slopes. The pipes were ruptured due to excessive water weight from the building site, causing the water to seep into the ground.
1993	<b>20<sup>th</sup> November:</b> <ul style="list-style-type: none"> <li>The road leading to Highland Towers started developing large cracks.</li> </ul> <b>11<sup>th</sup> December:</b> <ul style="list-style-type: none"> <li>At 1.40 p.m., Block 1 collapsed.</li> <li>The search and rescue operation involved the participation of 135 Federal Reserve Unit (FRU) members and around 35 military soldiers. Hundreds of police officers, firefighters, and rescue teams from the statutory body of Dewan Bandaraya Kuala Lumpur (DBKL) had arrived.</li> <li>Someone was seen brandishing a stick by the rescuers. A 23 years old maid and her 19 months old daughter were discovered at level 8.</li> <li>A Korean lady, 51, was rescued from the rubble but later declared dead due to severe internal brain bleeding.</li> <li>The Prime Minister and his teams visited the rubble location.</li> </ul> <b>12<sup>th</sup> December:</b> <ul style="list-style-type: none"> <li>After blocks 2 and 3 were deemed hazardous, the occupants were notified to depart. The Malaysian search and rescue teams received assistance from several Asian countries, such as Singapore, Thailand, Vietnam, Laos, Korea, and France. The Royal Malaysian Air Force (RMAF) also sent several helicopters to monitor the rescuing procedures from the air.</li> </ul> <b>13<sup>th</sup> December:</b> <ul style="list-style-type: none"> <li>The rescue effort was aided by a Korean group equipped with three rescue dogs. They excavated a hole four and a half metres deep and used heartbeat detectors to look for those still alive.</li> <li>The rescuer teams discovered seven corpses, four Japanese and two locals from Malaysia. The rescue teams brought several types of site machinery to demolish the concrete and steel to search for other victims that could be safe. Backhoes and bulldozers were used to clear the obstruction routes.</li> </ul> <b>18<sup>th</sup> December:</b> <ul style="list-style-type: none"> <li>The rescue mission was called off when the cabinet committee decided to give up.</li> </ul> <b>19<sup>th</sup> December:</b> <ul style="list-style-type: none"> <li>The rescuers discovered seven more corpses, including two kids.</li> </ul> <b>20<sup>th</sup> December:</b> <ul style="list-style-type: none"> <li>A woman was discovered at 8 p.m. in the parking lot area.</li> <li>A second woman located next to the first woman's corpse was found 30 min later.</li> <li>Two hours later, at 10.30 p.m., a man's corpse was discovered.</li> </ul> <b>22<sup>nd</sup> December:</b> <ul style="list-style-type: none"> <li>According to the police, 48 dead bodies were found in the rubble.</li> </ul> <b>23<sup>rd</sup> December:</b> <ul style="list-style-type: none"> <li>The search and rescue missions had been terminated.</li> </ul>

$$(3) \text{Overturning checking, } n = \frac{\sum H}{I} = \frac{123.52}{33.22} = 3.72 > 1.5 (\text{safe}) \quad (4)$$

$$(4) \text{Sliding checking, } J = \frac{\sum F}{\sum B} = \frac{39.19}{20.59} = 1.9 > 1.5 (\text{safe}) \quad (5)$$

Tables 4 and 5 shows Total  $\Sigma F = 39.19$  tonnes with  $\Sigma I_2 = 50.75$  tonnes.m. From all these values, the increased sum of force moments (I), eccentricity (M), and voltage can be obtained by calculating the following:

$$\sum I = I_1 - I_2 = 66.22 - 50.75 = 15.47 \text{ tonnes.m} \quad (6)$$

$$\text{Eccentricity, } M = \frac{\sum I}{\sum F} = \frac{\sum 15.47}{\sum 39.19} = 0.39 < \frac{1}{6}(b) = \frac{1}{6}(4) = 0.67 (\text{safe}) \quad (7)$$

$$N_{\max} = \frac{\sum F}{b} \left(1 + \frac{7.M}{b}\right) = \frac{39.19}{4} \left(1 + \frac{7 \times 0.03}{4}\right) = 10.31 \frac{\text{ton}}{\text{m}^2} < 20 \frac{\text{ton}}{\text{m}^2} (\text{safe}) \quad (8)$$

$$N_{\min} = \frac{\sum F}{b} \left(1 - \frac{7.M}{b}\right) = \frac{39.19}{4} \left(1 - \frac{7 \times 0.03}{4}\right) = 9.28 \frac{\text{ton}}{\text{m}^2} < 20 \frac{\text{ton}}{\text{m}^2} (\text{safe}) \quad (9)$$

Since the calculated  $N_{\min}$  and  $N_{\max}$  are  $9.28$  tonnes/m<sup>2</sup> and  $10.31$  tonnes/m<sup>2</sup>, they are determined that both values are safe since they are less than  $20$  tonnes/m<sup>2</sup>, which is allowed under land carrying capacity load.

#### 5.4. Strength stability

(1) Construction strength checking (Fig. 11)

$$N_{x1} = N_{\min} + \left(\frac{N_{\max} - N_{\min}}{b}\right)d = 9.28 + \left(\frac{10.31 - 9.28}{4}\right)1 = 9.54 \frac{\text{tonnes}}{\text{m}^2} \quad (10)$$

$$N_{x2} = N_{\min} + \left(\frac{N_{\max} - N_{\min}}{b}\right)(b - d) = 9.28 + \left(\frac{10.47 - 9.28}{4}\right)(4 - 1) = 8.39 \frac{\text{tonnes}}{\text{m}^2} \quad (11)$$

(2) Heel strength.

(a) Shear strength

$$O_1 = O_2 = O + P = 6 + 0.36 = 6.36 \text{m} \quad (12)$$

$$Q_1 = Q_2 = O_1 \times R_{\text{soil}} = 6.36 \times 1.57 = 10 \frac{\text{tonnes}}{\text{m}^2} \quad (13)$$

$$S_1 = S = S \times R_{\text{concrete}} = 2 \times 3.5 = 7 \frac{\text{tonnes}}{\text{m}^2} \quad (14)$$

$$N_{x1} = 9.54 \text{ tonnes/m}^2$$

$$N_{\min} = 9.28 \text{ tonnes/m}^2$$

$$T = Q_1 + S_1 - N_{x1} = 10 + 7 - 9.54 = 7.46 \quad (15)$$

$$U = Q_2 + S_2 - N_{\min} = 10 + 7 - 9.28 = 7.72 \quad (16)$$

$$V = \frac{1}{2} \times (T + U) \times d \times 1 = \frac{1}{2} \times (7.46 + 7.72) \times 1 \times 1 = 7.59 \text{ tonnes} \quad (17)$$

$$T = \frac{3}{2} \times \frac{V}{C \times 1} = \frac{3}{2} \times \frac{7.59}{2 \times 1} = 5.69 < 15 (\text{safe}) \quad (18)$$

$T = 5.69$  tonnes/m<sup>2</sup> is less than the allowable amount,  $T_{\text{allow}} = 15$  tonnes/m<sup>2</sup>. Hence, the retaining wall structure is secured against sliding.

(b) Tensile strength

$$W_1 = T \times d \times 1 = 7.56 \times 1 \times 1 = 7.56 \quad (19)$$

$$W_2 = \frac{1}{2} \times (U - T) \times d \times 1 = \frac{1}{2} \times (7.91 - 7.56) \times 1 \times 1 = 0.18 \text{ ton} \quad (20)$$

$$X = \left(W_1 \times \frac{1}{2} \times M\right) + \left(W_2 \times \frac{2}{3} \times M\right)$$

$$= \left(7.56 \times \frac{1}{2} \times 0.67\right) + \left(0.18 \times \frac{2}{3} \times 0.67\right) = 2.61 \text{ tonnes} \quad (21)$$



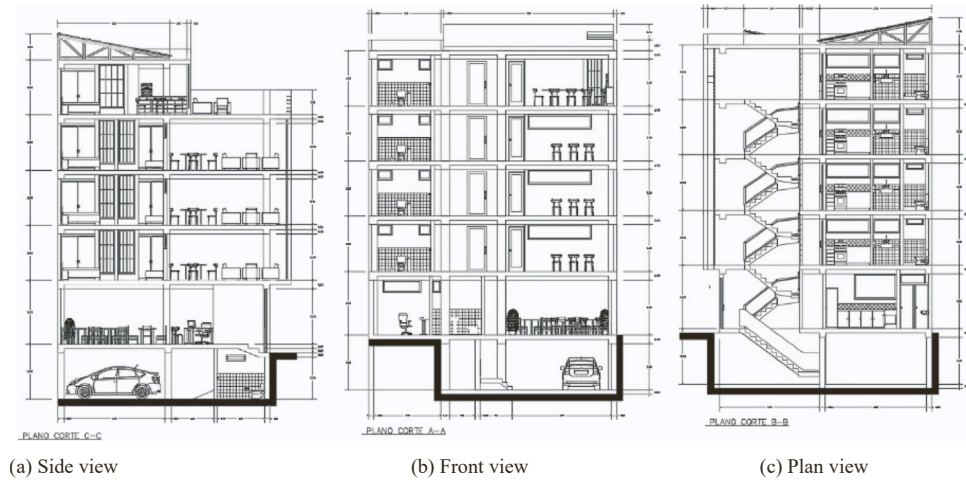


Fig. 4. Block 1's cross-section plan [18].

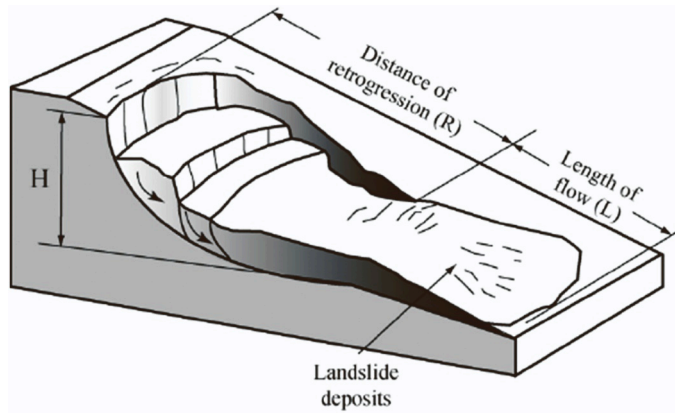


Fig. 5. Retrogressive landslide.

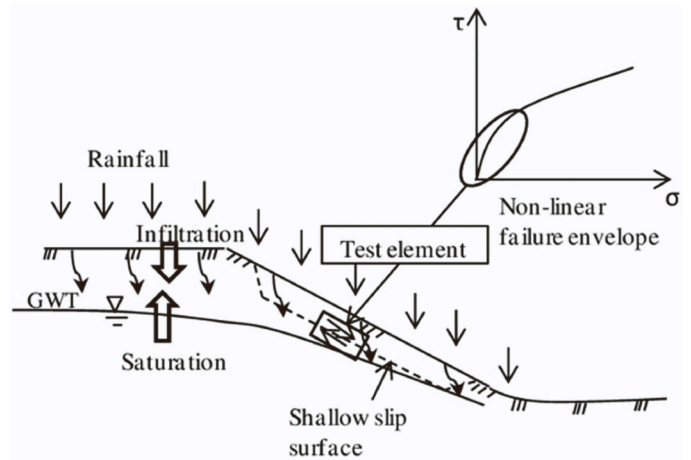


Fig. 7. Slope failure 2.

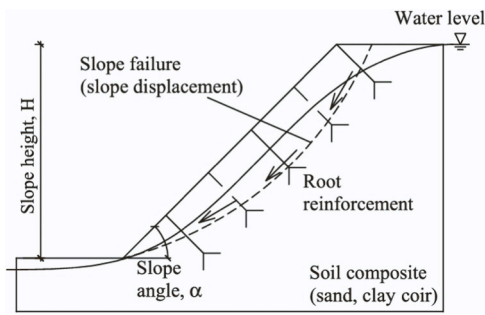


Fig. 6. Slope failure 1.

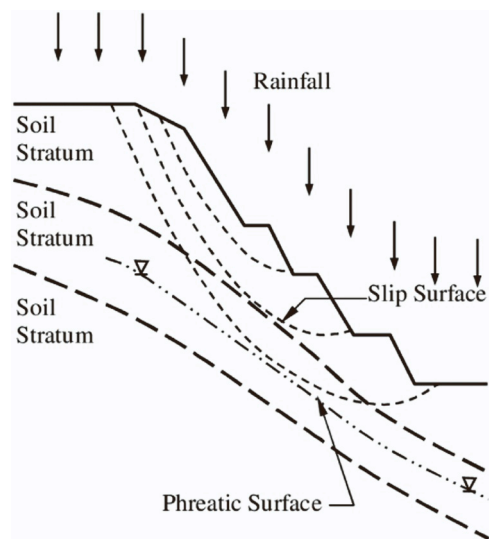


Fig. 8. Slope failure 3.

$$Y = \frac{1}{6} \times 1 \times 5^2 = \frac{1}{6} \times 1 \times 1^2 = 0.17\text{m}^3 \quad (22)$$

$$N = \frac{X}{Y} = \frac{2.61}{0.17} = 15.35 \frac{\text{tonnes}}{\text{m}^2} < 30 \frac{\text{tonnes}}{\text{m}^2} \text{ (safe)} \quad (23)$$

$N = 15.35 \text{ tonnes/m}^2$  is less than the allowable amount,  $N_{\text{allow}} = 30 \text{ tonnes/m}^2$ . So, it is secured and safe.

(3) Leg strength.

(a) Shear strength

$$O_1 = O_2 = 0.5\text{m}$$



Fig. 9. Gravity retaining wall.

Table 2  
Value details.

Detail	Value (m)
Peak width (a)	2
Width of foundation base (b)	4
Thickness of foot (c)	2
Width of foot (d)	1
Depth of foundation (e)	2
Foundation base to wall height (f)	7
Width of wall (g)	3

Parameters: A=Active soil coefficient, B=Horizontal force, R=Passive soil coefficient, C=Height of retaining wall, H=Active soil pressure, D=Arm turning point, F=Force, G=Arm facing point, H=Moment, I=Inertia, M=Eccentricity, N = Factor of safety, Q=Shear strength, T = Tensile strength, U=Ultimate strength, V=Velocity, W=Maximum load, X = Maximum pressure, Y=Maximum force, G=Maximum gravity

$$Q_1 = Q_2 = O_1 \times R_{soil} = 0.5 \times 1.57 = 0.79 \frac{\text{tonnes}}{\text{m}^2} \quad (24)$$

$$S_1 = S_2 = S \times R_{concrete} = 2 \times 3.5 = 7 \frac{\text{tonnes}}{\text{m}^2} \quad (25)$$

$$N_{x2} = 8.39 \frac{\text{tonnes}}{\text{m}^2}$$

$$N_{max} = 13.22 \frac{\text{tonnes}}{\text{m}^2}$$

$$T = N_{x2} - Q_1 + S_1 = 8.39 - 0.79 - 7 = 0.6(\text{up direction}) \quad (26)$$

$$U = N_{max} - Q_2 + S_2 = 13.22 - 0.79 - 7 = 5.43(\text{up direction}) \quad (27)$$

$$V = \frac{1}{2} \times (T + U) \times d \times 1 = \frac{1}{2} \times (0.6 + 5.43) \times 1 \times 1 = 3.02\text{tonnes} \quad (28)$$

$$T = \frac{3}{2} \times \frac{V}{c \times 1} = \frac{3}{2} \times \frac{3.02}{2 \times 1} = 2.27 \frac{\text{tonnes}}{\text{m}^2} < 15 \frac{\text{tonnes}}{\text{m}^2} (\text{safe}) \quad (29)$$

T = 2.27 tonnes/m<sup>2</sup> is less than the allowable amount, T<sub>allow</sub> = 15 tonnes/m<sup>2</sup>. Thus, the construction is secured from sliding.

(b) Tensile strength

$$W_1 = U \times d \times 1 = 5.43 \times 1 \times 1 = 5.43\text{tonnes} \quad (30)$$

$$W_1 = \frac{1}{2} \times (U - T) \times d \times 1 = \frac{1}{2} \times (5.43 - 0.6) \times 1 \times 1 = 2.42\text{tonnes} \quad (31)$$

Table 3  
Vertical force.

Symbol	Force (F) (ton)	Arm facing point (G) (m)	Moment (H) (ton.m) = F x G
W1	7	2.67	18.69
W2	13	3.5	45.5
W3	10.23	2	20.46
W4	7.69	4.46	34.3
W5	1.27	3.6	4.57
	ΣF= 39.19		ΣH= 123.52

Table 4  
Subsidence checking.

Symbol	Force (F) (ton)	Arm facing point (K) (m)	Moment (I <sub>2</sub> ) (ton.m) = F x K
F1	7	1.44	10.08
F2	13	1.5	19.5
F3	10.23	1	10.23
F4	7.69	1.06	8.15
F5	1.27	2.2	2.79
	ΣF= 39.19		ΣI <sub>2</sub> = 50.75

Table 5  
Body moment.

Symbol	Load (F) (tonnes)	Arm against point (G) (m)	Moment (H) = F x G
F1	7	1.44	10.08
F2	23	1.6	36.8
F3	7.85	2.2	17.27
	ΣF= 37.85		ΣH= 64.15

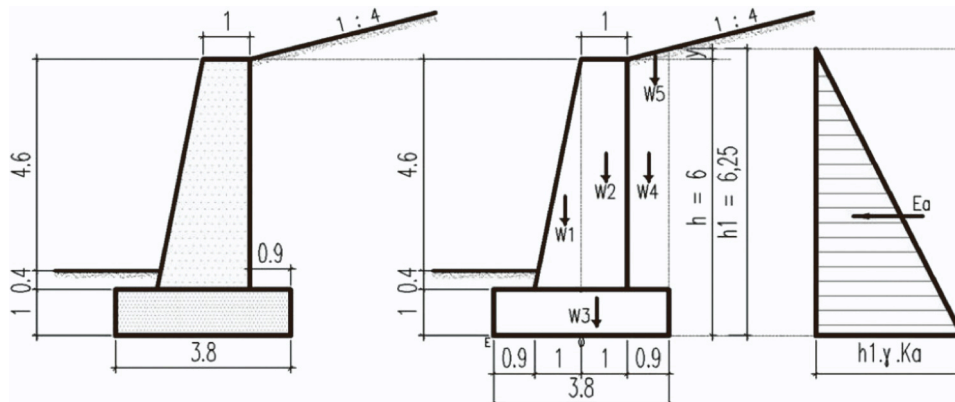


Fig. 10. Dimension (4–4.5 km).

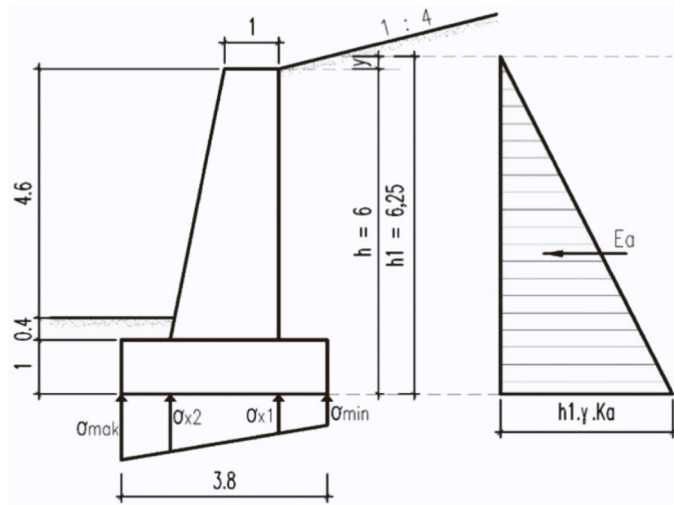


Fig. 11. Construction strength (4–4.5 km).

$$X = (W_1 \times \frac{1}{2} \times M) + (W_2 \times \frac{2}{3} \times M)$$

$$= (5.43 \times \frac{1}{2} \times 0.67) + (2.42 \times \frac{2}{3} \times 0.67) = 2.9 \text{tonnes} \quad (32)$$

$$Y = \frac{1}{6} \times 1 \times S^2 = \frac{1}{6} \times 1 \times 1^2 = 0.17 \text{m}^3 \quad (33)$$

$$N = \frac{X}{Y} = \frac{2.9}{0.17} = 17.06 < 30 \text{(safe)} \quad (34)$$

$N = 17.06 \text{ tonnes/m}^2$  is less than the allowable amount,  $N_{\text{allow}} = 30 \text{ tonnes/m}^2$ . Therefore, it is in a safe state.

$$I = I_A - I_B = 32.31 - 22.53 = 9.78 \text{tonnes.m} \quad (37)$$

$$G' = \frac{F}{A} + \frac{M}{\frac{1}{6} \times L \times C^2} = \frac{37.85}{3} + \frac{2.62}{\frac{1}{6} \times 2 \times 2^2} = 14.58 \frac{\text{tonnes}}{\text{m}^2}$$

$$< 150 \frac{\text{tonnes}}{\text{m}^2} \text{(safe)} \quad (38)$$

$$G' = \frac{F}{A} + \frac{I}{\frac{1}{6} \times L \times C^2} = \frac{37.85}{3} - \frac{2.62}{\frac{1}{6} \times 2 \times 2^2} = 10.65 \frac{\text{tonnes}}{\text{m}^2} < 30 \frac{\text{tonnes}}{\text{m}^2} \text{(safe)} \quad (39)$$

(4) Body strength (Fig. 12)

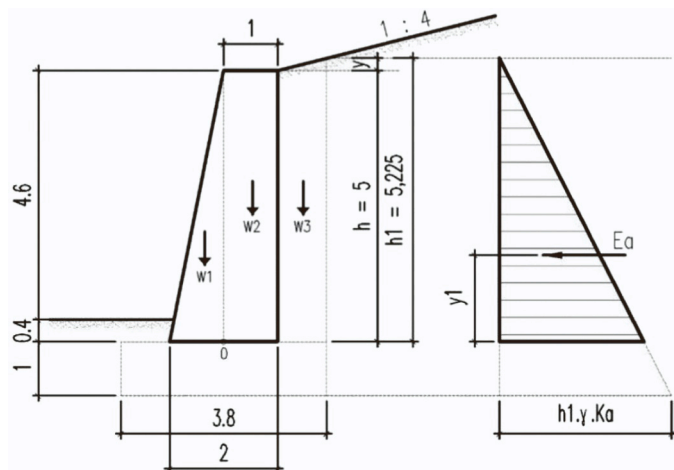


Fig. 12. Body strength (4–4.5 km).

$$P = \frac{1}{4} \times 1 = 0.25 \text{m}$$

$$D = \frac{1}{2} \times R \times O_1^2 \times A = \frac{1}{2} \times 1.57 \times 6.36^2 \times 0.48 = 15.24 \text{tonnes} \quad (35)$$

$$G = \frac{1}{3} \times 6.36 = 2.12 \text{m}$$

$$I_A = D \times G = 15.24 \times 2.12 = 32.31 \text{tonnes.m} \quad (36)$$

$G' = 14.58 \text{ tonnes/m}^2$  is less than the allowable amount,  $G'_{\text{allow}} = 150 \text{ tonnes/m}^2$  and another  $G' = 10.65 \text{ tonnes/m}^2$  is less than the permissible amount,  $G' = 30 \text{ tonnes/m}^2$ . Both values are proven to show that the design is safe.

5.2.1. Cantilever

A cantilever retaining wall refers to a wall that is not directly attached to the ground. A cantilever wall must be adequately designed since it retains a large soil volume. It is also the most typical retaining wall used in construction and is supported by a concrete slab below the surface. Instead of slab base weight, the weight of backfill and surcharge also prevents the wall from sliding and toppling over. Therefore, soil instability and landslide can be avoided and prevented. Steel, concrete or masonry is often in an inverted T shape and serves as an internal stem in a cantilever retaining wall. This wall transfers horizontal pressures from behind the wall as vertical pressures to the ground below. This pressure transfer increases the structural footing stability. In order to withstand heavy loads, the cantilever wall is sometimes buttressed at the front or has a counterfort at the rear. The buttress is an auxiliary wall projected outward from the main wall at a right angle. The concrete footing shall be set at a higher depth than the average seasonal frost depth to maintain stability. On the other hand, this cantilever retaining wall construction also requires less construction materials than gravity retaining wall. Figs. 13 and 14 demonstrates a cantilever retaining wall, while Fig. 13 illustrates the dimension of cantilever retaining wall.

$$k_a = \frac{1 - \sin K}{1 + \sin K} = \frac{1 - \sin 30^\circ}{1 + \sin 30^\circ} = \frac{1 - 0.5}{1 + 0.5} = \frac{1}{3} \quad (40)$$

$$\text{Active pressure, } A_a = k_a BC = \frac{1}{3} \times 20 \times 6.5 = 43.33 \frac{\text{kN}}{\text{m}^2} \quad (41)$$

Sliding.

Horizontal force acting on a 2 m wall length because of backfill factor:

$$\text{Wall weight, } E_w = 0.5 \times 6 \times 25 = 75 \text{kN, Base weight, } E_b = 0.5 \times 5 \times 25 = 62.5 \text{kN, Soil weight, } E_s = 3 \times 6 \times 20 = 360 \text{kN} \quad (42)$$

$$\text{Total vertical force, } E_t = 497.5 \text{kN}$$



Fig. 13. Cantilever retaining wall.



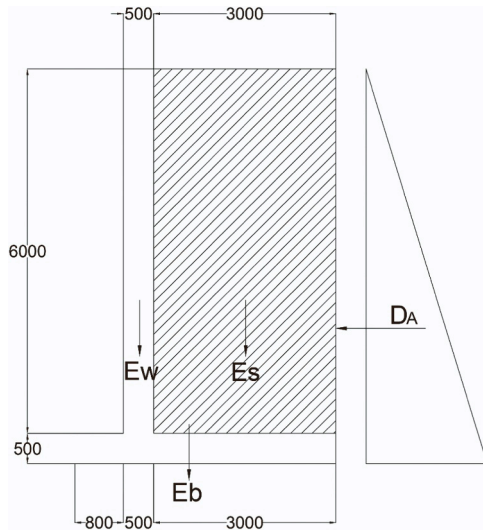


Fig. 14. Dimension.

$$\text{Friction force, } D_F = \lambda \mu E_t = 0.5 \times 497.5 = 248.75 \text{ kN} \quad (43)$$

$$\text{Passive pressure force, } D_p = 0, \text{ FOS} = \frac{248.75}{140.82} = 1.77 > 1.5, \text{ OK!} \quad (44)$$

#### Overturning

$$\text{Overturning moment, } G_{\text{over}} = \frac{D_A \times 6.5}{3} = \frac{140.82 \times 6.5}{3} = 30.11 \text{ kN.m} \quad (45)$$

$$\begin{aligned} \text{Restoring moment, } G_{\text{res}} &= (E_w \times 0.9) + (E_b \times 2) + (E_s \times 2.55) \\ &= (75 \times 0.9) + (62.5 \times 2) + (360 \times 2.55) \\ &= 1110.5 \text{ kNm} \end{aligned} \quad (46)$$

$$\text{Factor of Safety} = \frac{1110.5}{305.11} = 3.64 > 2, \text{ OK!} \quad (47)$$

#### Ground bearing pressure

$$\begin{aligned} \text{Moment, } G &= \left( \frac{D_A \times 5.4}{3} \right) + (E_w \times 1.1) - (E_s \times 0.55) \\ &= \left( \frac{140.82 \times 5.4}{3} \right) + (75 \times 1.1) - (360 \times 0.55) = 137.98 \text{ kNm} \end{aligned} \quad (48)$$

$$H = 472 \text{ kN}$$

$$\frac{G}{H} = \frac{137.98}{472} = 0.29 \text{ m} < \frac{I}{6} = \frac{5}{6} = 0.83 \text{ m} \quad (49)$$

$$\begin{aligned} \text{Maximum ground pressure, } B_{\text{toe}} &= \left( \frac{472}{5} \right) + \left( 6 \times \frac{137.98}{5^2} \right) = 127.52 \\ &< \text{allowable} \left( 130 \frac{\text{kN}}{\text{m}^2} \right) \end{aligned} \quad (50)$$

$$\begin{aligned} \text{Ground bearing pressure at heel, } A_{\text{heel}} &= \left( \frac{472}{5} \right) - \left( 6 \times \frac{137.98}{5^2} \right) \\ &= 61.28 \frac{\text{kN}}{\text{m}^2} \end{aligned} \quad (51)$$

#### Bending reinforcement.

##### Wall

$$\text{Height, } C_s = 6 \text{ m, } D_s = 0.5 k_a B C S^2 = 0.5 \times \frac{1}{3} \times 20 \times 6^2 = 120 \frac{\text{kN}}{\text{m}} \text{ width} \quad (52)$$

$$\text{Moment, } G = \frac{J_r D_s C_s}{3} = \frac{2.5 \times 120 \times 6}{3} = 600 \text{ kNm} \quad (53)$$

#### Effective depth

$$\begin{aligned} \text{Main steel diameter, } K &= 30 \text{ mm, Effective depth, } L = 400 - M - \frac{K}{2} \\ &= 400 - 40 - \frac{30}{2} = 345 \text{ mm} \end{aligned} \quad (54)$$

$$\begin{aligned} \text{Ultimate moment of resistance, } G_u &= 0.156 N_{cu} O L^2 \\ &= 0.156 \times 40 \times 15^3 \times 345^2 \times 10^{-6} \\ &= 2506.67 \text{ kNm} \end{aligned} \quad (55)$$

$$G_u > G, \text{ no compression reinforcement}$$

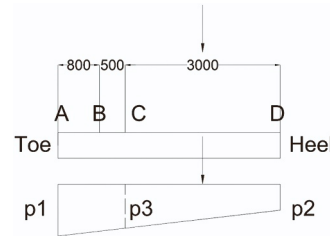
#### Steel area

$$P = \frac{G}{N_{cu} O L^2} = \frac{600 \times 10^6}{40 \times 15^3 \times 345^2} = 0.04 \quad (56)$$

$$Q = L \left( 0.5 + \sqrt{0.25 - \frac{P}{0.9}} \right) = 345 \left( 0.5 + \sqrt{0.25 - \frac{0.04}{0.9}} \right) = 328.92 \text{ mm} \quad (57)$$

$$\begin{aligned} F_s &= \frac{G}{0.87 N_y Q} = \frac{600 \times 10^6}{0.87 \times 600 \times 328.92} = 3494.54 \frac{\text{mm}^2}{\text{m}} \\ &= 0.13\% \text{ OC} = 0.13\% \times 15^3 \times 500 = 2913.75 \frac{\text{mm}^2}{\text{m}} \end{aligned} \quad (59)$$

#### Heel.



$$\begin{aligned} 360 \times 2.5 &= 900 \text{ kN, } B_1 = 2.5 \times 120 = 300 \frac{\text{kN}}{\text{m}^2}, B_2 = 2.5 \times 70 = 175 \frac{\text{kN}}{\text{m}^2}, B_3 \\ &= 175 + \left( \frac{3(300 - 175)}{5} \right) = 250 \frac{\text{kN}}{\text{m}^2} \end{aligned} \quad (60)$$

$$\begin{aligned} \text{Design moment, } G_c &= \left( \frac{900 \times 3}{3} \right) + \left( \frac{3 \times 49.5 \times 2.5 \times 2.56}{5} \right) - \left( \frac{175 \times 3^2}{3} \right) - \\ &\left( \frac{62.9 \times 3 \times 3}{3 \times 4} \right) = 900 + 190.08 - 525 - 47.18 \\ &= 517.9 \text{ kNm} \end{aligned} \quad (61)$$

$$\begin{aligned} \text{Assuming main steel diameter, } K &= 30 \text{ mm, } L = 400 - 55 - \frac{30}{2} = \\ &= 330 \text{ mm} \end{aligned}$$

$$P = \frac{517.9 \times 10^6}{40 \times 15^3 \times 330^2} = 0.04 \quad (62)$$

$$Q = 330 \left( 0.5 + \sqrt{0.25 - 0.0397/0.9} \right) \leq 0.95L = 0.95(330) = 313.5 \text{ mm} \quad (63)$$

$$F_s = \frac{G}{0.87 N_y Q} = \frac{517.9 \times 10^6}{0.87 \times 600 \times 313.5} = 3164.74 \frac{\text{mm}^2}{\text{m}} \quad (64)$$

#### Toe

$$\begin{aligned} \text{Design moment at point B, } M_B &\approx \frac{300 \times 0.8^2}{3} - \frac{0.8 \times 49.5 \times 2.5 \times 0.8}{5 \times 3} \\ &= 64 - 5.28 = 58.72 \text{ kNm} \end{aligned} \quad (65)$$

$$F_s = \frac{47.6 \times 2253}{517.9} = 207.07 \frac{\text{mm}^2}{\text{m}} < \text{minimum steel area} = 630 \frac{\text{mm}^2}{\text{m}} \quad (66)$$

**Reinforcement details.**

**5.3. Rock bolts installation**

(Fig. 15) Rock bolt is used as a support element in soil. The rock bolting design is primarily informed by empirical knowledge. It may seem that the rock bolting design is merely a matter of choosing rock bolt types and determining the bolt length and spacing. However, the specific methodology is explicitly or implicitly engaged in the rock bolting design process. This section provides a concise overview of the underlying design principles and methods used in rock bolting. These include the various types of rock bolts, design steps, methodologies utilisation and compatibility assessment between support elements.

**5.3.1. Wedge blocks at wall**

Fig. 16 shows the wedge blocks at a wall. Hoek and Brown (2018); Harrison and Hudson (2020) [41,42] introduced the concept of supporting wedge blocks at wall, as seen in Fig. 17(a). It is cited that a wedge-shaped block is presented within a wall and tends to undergo sliding motion below the discontinuity due to gravitational motion and force. It is protected using bolts that lie to the relative plane angle. The total force exerted=A, while the resulting force in a single rock bolt=a. Fig. 16(b) depicts the visual representation of various forces applied to the block. The forces exerted on the block include gravity force (B), bolt force (A), response force (C) and shear resistance force (D) on the sliding plane. During critical conditions, shear failure occurs, which shows that all forces are at an equilibrium state in all flows. By achieving equilibrium force, the normal force may be calculated by the following equation below:

$$C = A \sin \phi + B \cos \phi \quad (67)$$

The variable  $\phi$  represents the sliding plane angle. The expression of shear resistive force is based on the Mohr-Coulomb criteria dominated.

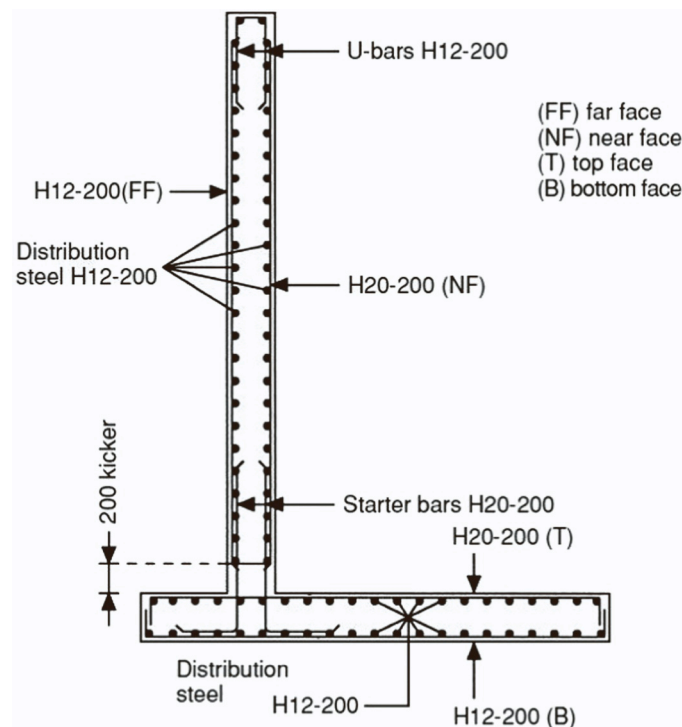


Fig. 15. Detailing.



Fig. 16. Wedge blocks at a wall.

$$D = EF + (A \sin \phi_1 + B \cos \phi_2) \tan \phi_3 \quad (68)$$

F = sliding plane base area, G = driving shear force:

$$G = B \sin \phi_2 - A \cos \phi_1 \quad (69)$$

Factor of safety (H) = shear resistance force (D) / driving shear force (G):

$$H = \frac{D}{G} = \frac{EF + (A \sin \phi_1 + B \cos \phi_2) \tan \phi_3}{B \sin \phi_2 - A \cos \phi_1} \quad (70)$$

$H < 1$  indicates the occurrence of sliding. Conversely, the block remains stable when  $H > 1$ . Rock bolting design often has a safety factor within the range of 2–3. The force exerted by the bolt (A) resulted in an augmentation of standard force as well as the constituent of shear force. The positive effect of increasing normal force on the frictional resistance of the sliding plane is well established. However, the impact of bolt force on shear force is contingent upon the installation angle ( $\phi_1$ ), either + or -. A theoretical critical installation angle ( $\phi_4$ ) has been identified and confirmed as the optimal orientation for bolts to produce maximum reinforcement in the block. In (70), let  $H = 1$ , which signifies the equivalent condition when shear and flexural failures are commenced along the sliding plane. The bolt force is determined as follows:

$$A = B \frac{\sin \phi_2 - \cos \phi_2 \tan \phi_3}{\cos \phi_1 + \sin \phi_1 \tan \phi_3} \quad (71)$$

The minimum bolt force required to increase the stability of alternate forces imposed on the block surface occurs when the tangential/angular velocity ( $\frac{\partial A}{\partial \phi_1} = 0$ ). The crucial installation angle is obtained by taking the given formula derivative concerning the  $\phi_1 = 0$ .

$$\phi_3 = \phi_4(6)$$

In alternative terms, the optimal reinforcing effect of rock bolts is highly achieved when they are located and positioned at a specific angle.

**5.3.2. Arching bolting**

The elucidation of the natural pressure arch notion is facilitated by the arching phenomenon observed in the two block arrangements, as depicted in Fig. 18. An excavation has been made in a rock mass with layers, and the uppermost part of this excavation consists of two distinct blocks that have been generated due to three cracks that emerged across the roof stratum. The low displacement prevention of the two blocks is attributed to frictional forces acting on the fracture planes. Subsequently, due to the influence of gravitational forces, the two blocks undergo rotational motion and exert pressure on each other. Specifically, this pressure occurs at abutment and central fracture plane sections. Consequently, a pressure arch is generated between the two blocks, making them more stable. The original pressure arch is significantly situated from the subterranean aperture ceiling when the

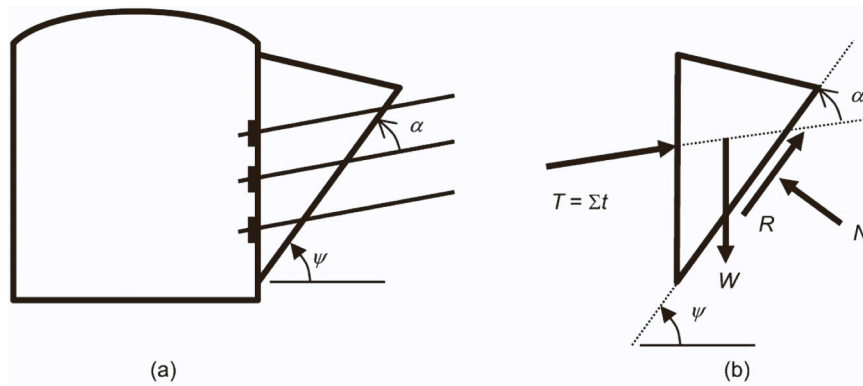


Fig. 17. (a) Block + rock bolts (b) Forces.

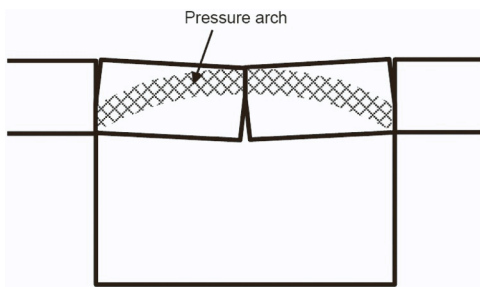


Fig. 18. Two ceiling blocks.

substantial failure zone is formed around the excavation opening. It is plausible to contemplate the implementation of an unnatural pressure arch within the uncompleted area to avert the descent of fractured rocks. The formation of abnormal pressure arches in the systematically implanted rock bolts had been proven in physical simulations conducted by Lang (2016); Hoek (2017) [43,44], as delineated in Fig. 19. The arch pressure load-bearing capacity can also be evaluated using the experimental research data from Krauland (2023); Sinha (2019) [45,46].

$$\sigma_{max} = I\sigma_u \left(\frac{J}{K}\right)^2 \tag{72}$$

The variable  $\sigma_{max}$  represents the upper limit of ground pressure that the pressure arch can withstand. Subsequently,  $\sigma_u$  denotes the rock mass's uniaxial compressive strength (UCS) strengthened by bolts. The

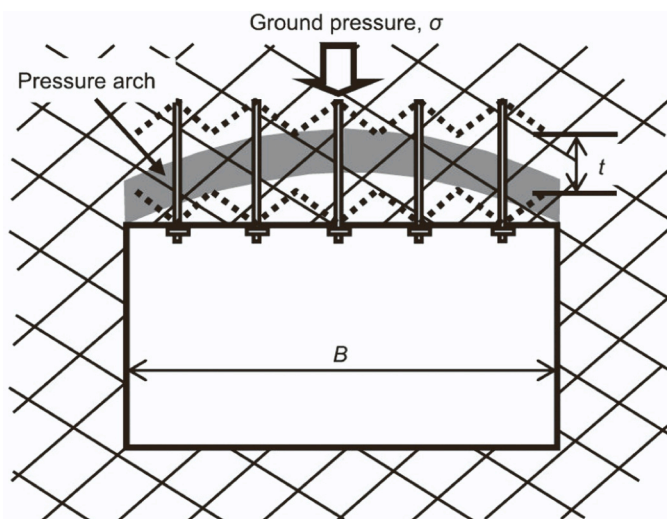


Fig. 19. Bolt-reinforced roof.

coefficient I exhibits a direct proportionality with the moment arm length within the pressure arch. The I value was determined to be one according to the design calculation steps [47].

5.3.3. Tieback bolting

Rock pillars are commonly used in tieback bolting. Tieback bolting involves using bolts that are in a pre-tensioned state with a reasonably high load and placed over the pillar width (Fig. 20). It's important to keep in mind that tieback bolting isn't meant to increase the pillar's peak strength to avoid failure but rather to keep the pillar together after it fails. The Mohr-Coulomb method expresses the rock strength inflation based on confining pressure  $s_3$  as indicated below:

$$\Delta\sigma_1 = \sigma_3 \tan^2\left(45^\circ + \frac{\alpha}{2}\right) \tag{73}$$

Consider a pillar fortified with tieback bolts having a 2 m spacing interval. The maximum confining stress imposed on the rock by the bolts is 0.3 MPa with 300 kN ultimate load. The internal friction angles at peak and residual are  $40^\circ$  and  $50^\circ$ , respectively. The enhanced peak and residual strengths are 0.7 MPa and 1 MPa, which are determined from Eq. (8). Normally, rocks have a UCS over 60 MPa. 0.9 MPa strength rise is more significant than the rock's innate strength. Nevertheless, most rock types have weak and unconfined residual strength. Thus, if 0.7 MPa could increase the pillar's residual strength, its behaviour after failure would be enhanced. A hydroelectric plant wall is excavated to create two niches, each measuring 7 m ( $w$ ) x 9 m ( $d$ ), as delineated in Fig. 21. The excavating process caused an extension fracture in the pillar. 2 MN-rated cable bolts were installed at 3 m spacing across the pillar with 500 kN pre-tensioned force. 400 mm concrete cover thickness was cast on both pillars to increase and ensure the weight transmission efficiency from cable bolts to pillar achieves the highest rate. The cable fasteners were strengthened and reinforced with 300 mm x 300 mm square

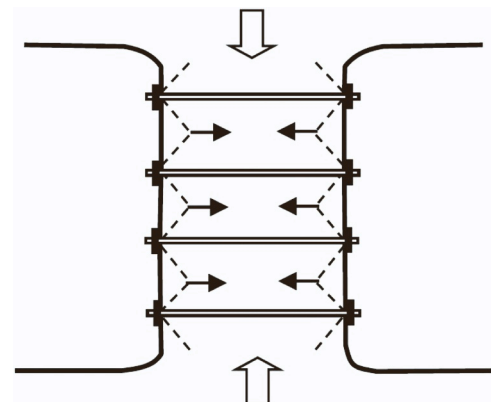


Fig. 20. Tieback bolting.



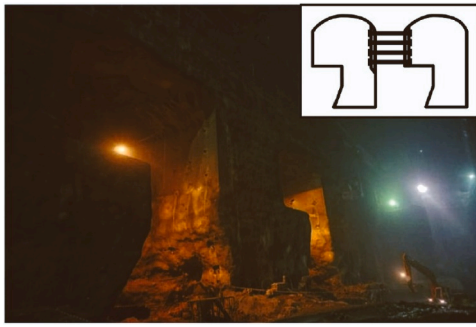


Fig. 21. Pillar cable bolting.

plates. Besides that, the cable bolts produce a maximum confining pressure of about  $2 \text{ MN}/(3 \text{ m} \times 3 \text{ m}) = 0.22 \text{ MPa}$ . For a  $7 \text{ m} \times 9 \text{ m}$  pillar, the load capacity increases from  $25 \text{ MN}$  to  $37 \text{ MN}$  with  $40^\circ$  internal friction angle and  $0.8 \text{ MPa}$  estimated increase in pillar strength.

#### 5.3.4. Suspension bolting

The ceiling of mine drifts can sometimes reveal a weak layer formation, especially in coal mines [48]. As demonstrated in Fig. 22, rock bolts can be used to suspend this layer from the solid layer below. Since the weak layer is loaded by weight, the bolting design may be solely based on the thickness and distance between bolts. The rock bolts' ultimate load capacity shall be able to support the imposed load on the surface.

$$P_{ult} = HMEP(9.81) \tag{74}$$

where  $M$ =vulnerable layer thickness,  $E$  = row-to-row bolt spacing. The bolt length must be at least ( $L_{min}$ ):

$$L_{min} = M + N \tag{75}$$

When using wholly enclosed bolts, the stable stratum's anchoring length ( $N$ ) must be at least  $2 \text{ m}$ . It has to be  $3$ – $5$  times long as well as the minimum necessary embedment length.

#### 5.4. Vegetative plantation

Soil conservation techniques and plant growth that penetrate the chronically extensive tree layers are two ways to combat landslide [49]. To achieve this goal, one must consider the unique characteristics of trees and the ideal soil condition. For instance, roots need to be extremely wide, robust, and deep to close the ground rapidly and produce dense hybrid breeding development [50]. Moreover, the crop shall have a water-volatile feature, which is helpful in the future if planted in rainy regions [51]. Several green plants can be planted on the ground to

reduce landslide. *Tamarindus Indicus*, *Cinnamomum Zeylanicum*, *Asparagus Cochinchinensis*, *Durio zibethinus* [52–54], and the like are all viable plant options. *Ageratum Conizoides* and ground cover strata, such as *Chrysopogon zizanioides*, *Pennisetum Purpureum*, and *Megathyrus maximus* [55–57] are the other plant options available. All these green plants with bush strata are highly recommended to be chosen for planting. According to Wudianto and Rini (2019) [58], this closure crop can be considered a supplementary measure to minimise landslip risks. Also, it can improve and enhance soil structure, boost organic matter, stop nutrient leaching, lower soil temperatures, and increase organic substances. Table 6 describes the 15 types of green plant details that can be planted to prevent landslide. All these 15 green plants have unique characteristics and properties. Each green plant has different structures, either trees, shrubs or ground cover. Their growing tolerant ranges are also different from each other, which were  $600$ – $3100$ . Most green plants have a growing tolerant range of less than  $2000$ . The dimension is also different from each other. From Table 6, *Pangium edule Reinw* has the biggest dimension ( $65 \text{ m} \times 1.3 \text{ m} \times 19 \text{ m}$ ), while *Ageratum conyzoides* has the smallest size ( $0.7 \text{ m} \times 0.5 \text{ m} \times 0.2 \text{ m}$ ). There are two types of roots available. Nine green plants have radix primaria root type, while the other six have radix adventicia root type. Both roots have the same strength, characteristics and properties to strengthen the soil properties, preventing landslide. All green plant roots and leaves have densities. The densities are essential because they can absorb excessive water in the soil. The green plants' primary role is crucial in protecting healthy soil. In addition, they also help to prevent soil erosion because their roots and the microorganisms that dwell in and around them bind the soil together and firmly. When these 15 green plants become old and eventually die, their leaves will fall on the ground, causing disintegration, soil enrichment and allowing for the growth of new green plants.

Natural plants grown in unstable locations may include trees over  $30$  and even over  $110$  years old. Agricultural usage is discouraged on slopes steeper than  $20^\circ$ , but natural perennials are suitable for growing there. In addition to acting as a protective layer for the soil, the chosen plant species should also enhance soil structure, reduce the rate at which nutrients are leached out of the ground, and increase the amount of organic matter in the soil. This vegetative engineering method should diminish the kinetic energy of falling raindrops and ground surface flows. The data suggests that plants with sturdy stems and roots that can retain water are most likely to survive avalanches. Root density is one of the essential factors in landslip resistance. Table 1 lists two plant species that meet those criteria: fibre roots (*Radix Adventicia*) and tail roots (*Radix Primaria*). Dicotyledonous is the most common plant that has tap roots. Root riding refers to a kind of root continuously developing from the outward roots. They are also known as wild roots since they are not included in the initial root growth. *Radix Adventicia* are also named because of their atypical appearance and fibre content characteristics. Grass is also a monocotyledonous plant with thin and fibrous roots and it has tapering leaves that grow up on the stem. Also, soil erosion and landslide can be avoided because the natural fibrous fibre network absorbs water. When the water content in the soil declines, the soil microstructures become stronger by inclining the compression and tension forces with each other [59–62]. All the fifteen plants in Table 1 are suitable to be planted and grown at  $0$ – $3000 \text{ m}$  altitude above sea level, as required by vegetative plantation criteria standards. The criteria for classifying shrubs and ground cover plants are also included, as well as the fifteen plant species in Table 1, which have been evaluated for their potential to reduce and even eliminate landslip incidents due to their excellent rooting microstructures [63–78].

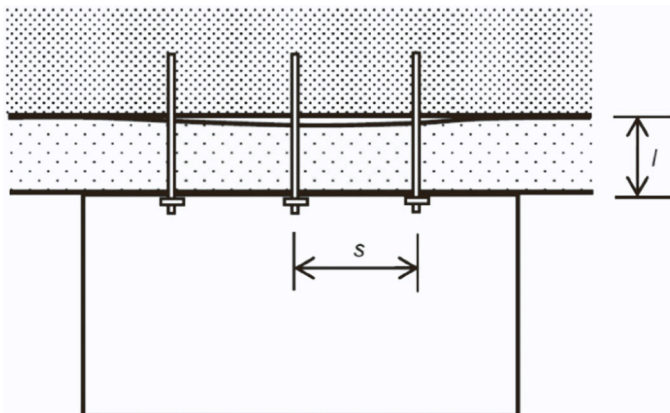

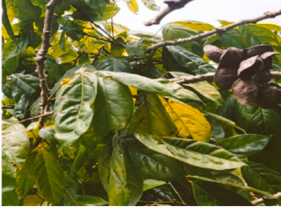




Fig. 22. Suspension bolting.

## 6. Conclusion





In conclusion, possible causes of Block 1, Highland Towers condominium collapse, are poor drainage, retaining wall failure, and rail piling foundation. Human mistake is shown to play a predominant role in causing the landslide to occur. In addition to technological

**Table 6**  
15 types of green plant details that can be planted to prevent landslide.

No	Green plant scientific name	Structure			Growing tolerant range	Dimension: height (m) x header (m) x diameter (m)	Root		Density	
		Tree	Shrubs	Ground Cover			Radix primaria	Radixadv enticia	Root	Leaf
1	Aleurites Mollucana	Yes	No	No	600–1300	45 × 2×35	Yes	No	Yes	Yes
										
2	Archidendron Pauciflorum	Yes	No	No	1100	27 × 4×15	Yes	No	Yes	Yes
										
3	Swietenia Macrphylla	Yes	No	No	< 1600	26 × 1.3 × 9	Yes	No	Yes	Yes
										
4	Dalbergia Soides	Yes	No	No	< 700	35 × 2×8	Yes	No	Yes	Yes
										

(continued on next page)






Table 6 (continued)

No	Green plant scientific name	Structure			Growing tolerant range	Dimension: height (m) x header (m) x diameter (m)	Root		Density	
		Tree	Shrubs	Ground Cover			Radix primaria	Radixadv enticia	Root	Leaf
5	Tamarindus Indicus	Yes	No	No	< 1600	35 × 3×16	Yes	No	Yes	Yes
										
6		Yes	No	No	600–1600	16 × 3×16	Yes	No	Yes	Yes
										
7	Asparagus Cochinchinensis	Yes	No	No	900–1100	23 × 0.7 × 23	No	No	Yes	Yes
										
8	Durio zibethinus	Yes	No	No	< 900	36 × 5×13	Yes	No	Yes	Yes
										

(continued on next page)





Table 6 (continued)

No	Green plant scientific name	Structure			Growing tolerant range	Dimension: height (m) x header (m) x diameter (m)	Root		Density	
		Tree	Shrubs	Ground Cover			Radix primaria	Radixadv enticia	Root	Leaf
9	Cupressus Lusitanica	Yes	No	No	300–2100	45 × 3×7	No	Yes	Yes	Yes
										
10	Agathis dammara	Yes	No	No	400–1300	40 × 1.7 × 20	Yes	No	Yes	Yes
										
11	Pangium edule Reinw	Yes	No	No	< 1300	65 × 1.3 × 19	Yes	No	Yes	Yes
										
12	Ageratum conyzoides	No	Yes	No	2–2200	0.7 × 0.5 × 0.2	No	Yes	Yes	Yes
										
13	Chrysopogon zizanioides	No	Yes	No	600–1600	3 × 2×1.5	No	Yes	Yes	Yes
										

(continued on next page)

Table 6 (continued)

No	Green plant scientific name	Structure			Growing tolerant range	Dimension: height (m) x header (m) x diameter (m)	Root		Density	
		Tree	Shrubs	Ground Cover			Radix primaria	Radix adventicia	Root	Leaf
14	Pennisetum Purpureum	No	No	Yes	1–3100	2 × 3×5	No	Yes	Yes	Yes
										
15	Megathyrus maximus	No	No	Yes	< 2000	4 × 6×1	No	Yes	Yes	Yes
										

advancements, it is essential to remember that a structure's design, building, and maintenance must have sufficient quality to ensure its dependability. In order to minimise human mistakes, it is advisable to do a human reliability analysis during slope development to prevent landslide disasters. This case study supports and acknowledges the viability of dependability theory as a logical alternative. A gravity retaining wall may be built behind the Block 1, Highland Towers condominium in order to stabilise the slope, which is made up of clay gravel soil. The proposed dimension of the retaining wall is 7 m (h) x 1 m (w) x 3 m (t). The proposed foundation's (w) x (t) is 4 m x 2 m, while the dimension for peak body width should be 2 m. The retaining wall's stability has been assessed and poses no collapse, movement, or subsidence risk. The rocks above and around the underground excavation form a genuine pressure arch beyond the failure zone. Installing short and tight rock bolts and securing long cables in the existing pressure arch in the failure zone create an abnormal pressure arch. Focusing on rock bolts having the same displacement and energy absorption capability as the other support parts is vital when designing a rock support system. Vegetative plantation involves growing certain plant types like trees, shrubs, and ground cover layers. This vegetative plantation is vital because it can mitigate landslip hazards and risks. Finally, communities and government agencies in landslide-prone regions shall adopt this vegetative plantation approach to reduce the landslide disaster risk.

## 7. Recommendations

(1) The gravity retaining wall shall be constructed to prevent landslide from occurring, which can save many innocent people's lives.

(2) There are four method types of rock bolt installations. All these four methods are crucial and must be installed on the ground surface to increase the soil stability.

(3) Vegetative plantation is also one of the most essential methods in preventing landslide. Fifteen plant types can be planted on the ground surface. At least eight to ten plant species shall be planted in order to enhance the soil structure, boost organic matter, stop nutrient leaching, lower soil temperatures, and increase organic substances, which can prevent landslide in future.

## Declaration of Competing Interest

The authors declare that they have no known competing financial interests or personal relationships that could have appeared to influence the work reported in this paper.

## References

- [1] Gue, S.S. and S.Y. Wong, 2018. How to Improve Slope Management and Slope Engineering Practices in Malaysia. Retrieved from: ([www.gnpgeo.com.my](http://www.gnpgeo.com.my)).
- [2] JKR, 2009. Final Investigation Report Investigation of Slope Failure at Taman Bukit Mewah. Bukit Antarabangsa Hulu Klang Salengor. Cawangan Kejuruteraan Cerun, Jabatan Kerja Raya Malaysia. 1.
- [3] JKR, 2009. National Slope Master Plan. Sectoral Report Research and Development, Jabatan Kerja Raya Malaysia.
- [4] Gue, S.S. and Y.C. Tan, 2016. Landslide: Cases Histories, Lessen Learned and Mitigation Measures. Paper Presented at the Landslide, Sinkhole, and Structure Failure: Myth or Science? Ipoh, Malaysia.
- [5] M.S. Reis, G. Gins, Industrial process monitoring in the big data/industry 4.0 era: from detection, to diagnosis, to prognosis, *Processes* 5 (3) (2017) 35.
- [6] J. Wang, W. Ip, R.R. Muddada, J. Huang, W. Zhang, On Petri net implementation of proactive resilient holistic supply chain networks, *Int. J. Adv. Manuf. Technol.* 69 (2013) 427–437.
- [7] A. Khodabakhsh, I. Ari, M. Bakir, A.O. Ercan, Multivariate sensor data analysis for oil refineries and multi-mode identification of system behavior in real-time, *IEEE Access* 6 (2018) 64389–64405.
- [8] Q.P. He, J. Wang, Statistical process monitoring as a big data analytics tool for smart manufacturing, *J. Process Control* 67 (2018) 35–43.
- [9] J. Ren, D. Ni, A batch-wise lstm-encoder decoder network for batch process monitoring, *Chem. Eng. Res. Des.* 164 (2020) 102–112.
- [10] R. Behmanesh, I. Rahimi, Using combination of optimised recurrent neural network with design of experiments and regression for control chart forecasting, in: *Business Engineering and Industrial Applications Colloquium*, vol. 1, 2012, pp. 435–439.
- [11] V. Gundu, S.P. Simon, Pso-lstm for short term forecast of heterogeneous time series electricity price signals, *J. Ambient Intell. Humaniz. Comput.* 12 (2) (2021) 2375–2385.
- [12] N.M. Newmark, Effects of earthquakes on dams and embankments, *Geotechnique* 15 (2) (1965) 139–160, <https://doi.org/10.1680/geot.1965.15.2.139>.
- [13] F.I. Makdisi, H.B. Seed, Simplified procedure for estimating dam and embankment earthquake-induced deformations, *ASCE J. Geotech. Eng. Div.* 104 (7) (1978) 849–867, <https://doi.org/10.1061/ajgeb6.0000668>.
- [14] J.D. Bray, E.M. Rathje, Earthquake-induced displacements of solid-waste landfills, *J. Geotech. Geoenviron. Eng.* 124 (3) (1998) 242–253, [https://doi.org/10.1061/\(asce\)1090-0241\(1998\)124:3\(242\)](https://doi.org/10.1061/(asce)1090-0241(1998)124:3(242)).

- [15] E.M. Rathje, J.D. Bray, An examination of simplified earthquake-induced displacement procedures for earth structures, *Can. Geotech. J.* 36 (1) (1999) 72–87, <https://doi.org/10.1139/98-076>.
- [16] R.W. Jibson, E.L. Harp, J.A. Michael, A method for producing digital probabilistic seismic landslide hazard maps, *Eng. Geol.* 58 (3–4) (2000) 271–289.
- [17] J.D. Bray, T. Travasaru, Simplified procedure for estimating earthquake-induced deviatoric slope displacements, *J. Geotech. Geoenviron. Eng.* 133 (4) (2007) 381–392, [https://doi.org/10.1061/\(asce\)1090-0241\(2007\)133:4\(381\)](https://doi.org/10.1061/(asce)1090-0241(2007)133:4(381)).
- [18] Franklin A.G., Chang F.K. Miscellaneous Paper. Earthquake resistance of earth and rock-fill dams, S-7vols. 1–17. Vicksburg, Miss: US Army Corps of Engineers Waterways Experiment Station; 1977.
- [19] N.N. Ambraseys, J.M. Menu, Earthquake-induced ground displacements, *Earthq. Eng. Struct. Dynam* 16 (7) (1988) 985–1006, <https://doi.org/10.1002/eqe.4290160704>.
- [20] R.W. Jibson, Regression models for estimating coseismic landslide displacement, *Eng. Geol.* 91 (2–4) (2007) 209–218, <https://doi.org/10.1016/j.enggeo.2007.01.013>.
- [21] E.M. Rathje, G. Antonakos, A unified model for predicting earthquake-induced sliding displacements of rigid and flexible slopes, *Eng. Geol.* 122 (1–2) (2011) 51–60, <https://doi.org/10.1016/j.enggeo.2010.12.004>.
- [22] JKR (2009) National slope master plan sectoral report research and development, Jabatan Kerja Raya Malaysia.
- [23] Schüttrumpf H., Kortenhaus A., Fröhle P., Peters K. (2008) Analysis of uncertainties in coastal structure design by expert judgement. In: Proceedings of the Chinese-German Joint Symposium on Hydraulic and Ocean Engineering: August 24–30, 2008, Technische Universität Darmstadt/Publ. by the Institute of Hydraulic and Water Resources Engineering, pp 109–114.
- [24] Holger, S., K. Andreas, F. Peter and P. Karsten, 2008. Uncertainties in Coastal Structure Design by Expert Judgement. Chinese-German Joint Symposium on Hydraulic and Ocean Engineering, August 24–30, 2008, Darmstadt.
- [25] G. Reichart, How to reduce Design and Construction errors, *Nucl. Eng. Des.* 110 (2) (1988) 251–254.
- [26] Ngeue, C.S., 2006. Case studies on forensic structural engineering. M.Sc. Thesis, Civil Engineering, Universiti Teknologi, Malaysia.
- [27] Fatt, C.S. and Y.S. Fang, 2009. Study of the Rainfall Characteristics of Bukit Antarabangsa Area In Relation To The Landslide Incident on 6th December 2008. 11th Annual IEM Water Resources Colloquium 2009.
- [28] Harahap, I.S.H. and F. Aini, 2010. On Aspects of Geotechnical Risk Assessment for Hillside Development. International Conference on Sustainable Building and Infrastructure (ICSBI2010) Kuala Lumpur, Malaysia.
- [29] Fatt, C.S. and Y.S. Fang, 2009. Study of the Rainfall Characteristics of Bukit Antarabangsa Area In Relation To The Landslide Incident on 6th December 2008. 11th Annual IEM Water Resources Colloquium, 2009.
- [30] J. Lee, H. Lee, H. Yun, C. Kang, M. Song, Improved vulnerability assessment table for retaining walls and embankments from a working-level perspective in Korea, *Sustainability* vol. 13 (3) (2021) 1–23, <https://doi.org/10.3390/su13031088>.
- [31] B.G. dan, G. Sandjaja, Analisis Ulang Dinding Penahan Tanah Dengan Pendekatan Perhitungan Manual Yang Memperhitungkan Akibat Beban Gempa, *J. Mitra Tek. Sipil* vol. 2 (3) (2019) 43–52.
- [32] X. Li, S. Zhao, S. He, Q. Yan, X. Lei, Seismic stability analysis of gravity retaining wall supporting c-φ soil with cracks, *Soils Found.* vol. 59 (4) (2019) 1103–1111, <https://doi.org/10.1016/j.sandf.2019.01.004>.
- [33] R.R. Djunaedi, Perencanaan Dinding Penahan Tanah Tipe Gravitasi (Studi Kasus: SDN Lio, Kecamatan Cireunghas), *J. Stud. Tek. Sipil* vol. 2 (1) (2020) 55–64.
- [34] X. Guan, G.S.P. Madabhushi, Dynamic response of a retaining wall with a structure on the dry backfill, *Soil Dyn. Earthq. Eng.* vol. 157 (June 2021) (2022), 107259, <https://doi.org/10.1016/j.soildyn.2022.107259>.
- [35] R. Tiwari, N. Lam, Modelling of seismic actions in earth retaining walls and comparison with shaker table experiment, *Soil Dyn. Earthq. Eng.* vol. 150 (August) (2021), 106939, <https://doi.org/10.1016/j.soildyn.2021.106939>.
- [36] P. Xu, K. Hatami, G. Jiang, Seismic rotational stability analysis of reinforced soil retaining walls, *Comput. Geotech.* vol. 118 (October 2019) (2020), 103297, <https://doi.org/10.1016/j.compgeo.2019.103297>.
- [37] A.P. DM, R. Wirawan, Perencanaan Pencegahan Tanah Longsor dengan Metode Dinding Penahan Tanah, *J. Karajata Eng.* vol. 3 (1) (2023) 59–63.
- [38] E.S. Tjhan, Pengaruh Gempa Terhadap Dinding Penahan Tanah Tipe Kantilever, *J. Ilm. Media Eng.* vol. 9 (1) (2019).
- [39] B.M. Das, Principles of Geotechnical Engineering, Cengage learning, 2021.
- [40] B. Surendro, Rekayasa Fondasi, Teori dan Penyelesaian, Graha Ilmu, Yogyakarta, 2014.
- [41] E. Hoek, E.T. Brown, Underground excavations in rock, Institution of Mining and Metallurgy, London, 2018.
- [42] P. Harrison, J. Hudson, Engineering rock mechanics. Part 2: illustrative worked examples, Pergamon, 2020.
- [43] Lang T.A. Theory and practice of rockbolting. Transactions of American Institute of Mining, Metallurgical, and Petroleum Engineers 2016;220:333e48.
- [44] Hoek E. Model to demonstrate how bolts work. In: Practical rock engineering; 2017.
- [45] N. Krauland, Rockbolting and economy, in: O. Stephansson (Ed.), Rockbolting Theory and Applications in Mining and Underground Construction, A.A. Balkema, Rotterdam, 2023, p. 499e507 (p.).
- [46] R.S. Sinha, Rock reinforcement. In: Underground structures e design and instrumentation, Elsevier, Amsterdam, 2019, p. 129e58.
- [47] F.D. Wright, Roof control through beam action and arching, in: SME Mining Engineering Handbook, vol. 1, Society of Mining Engineers, New York, 2023, p. 80e 96. Chapter 13.
- [48] C.O. Aksoy, T. Onargan, The role of umbrella arch and face bolt as deformation preventing support system in preventing building damages, *Tunn. Undergr. Space Technol.* 25 (5) (2010) 553e9.
- [49] Detik.com 2017 Dahsyatnya Bencana Longsor di Ponorogo (<https://news.detik.com/berita-jawatimur/d-3462400/dahsyatnya-bencana-longsor-di-ponorogo-ini-enampakannya>) (Accessed 17 October 2017).
- [50] Riyanto and Dwi H. 2016 Rekayasa Vegetatif Untuk Mengurangi Risiko Longsor (Surakarta: Balai Penelitian Pengembangan Teknologi Pengelolaan Daerah Aliran Sungai).
- [51] Sarief E. and Saifuddin 1985 Konservasi Tanah dan air (Bandung: Penerbit Pustaka Buana).
- [52] Hardiyanto, H. Christady, Tanah Longsor dan Erosi, Kejadian dan Penanganan, Gadjah Mada University Press, Yogyakarta, 2012.
- [53] T.W. Daniel, J.A. Helms, F.S. Baker, Prinsip-Prinsip Silvikultur, Gadjah Mada University Press, Yogyakarta, 1987.
- [54] Hardjowigeno and Sarwono 1987 Ilmu Tanah (Jakarta: PT Mediyatama Sarana Perkasa).
- [55] Highland L. 2004 Landslide type and processes, act-Sheet No. 2004–3073, July 2004 (US: Geological Survey).
- [56] Pusat Ilmu Geografi Indonesia 2015 13 Penyebab Tanah Longsor dan Penanggulangannya (<https://ilmugeografi.com/ilmu-bumi/tanah/penyebab-tanah-longsor/>) (Accessed 9 November 2017).
- [57] Sastrahidajat and Rochdjatun I. 1991 Budidaya Tanaman Tropika (Surabaya: Penerbit Usaha Nasional).
- [58] Wudianto and Rini 1990 Mencegah Erosi (Jakarta: Penerbit Penebar Swadaya).
- [59] S. Azar, R.M.Z. Subhi, A.S. Abdurraheem, R.R. Zebari, A.M.S. Mohammed, M. A. Omar, Evolution of mobile wireless communication to 5G Revolution, *Technol. Rep. Kansa Univ.* vol. 62 (5) (2019) 2139–2151.
- [60] A. Srivastava, M.S. Gupta, G. Kaur, Energy efficient transmission trends towards future green cognitive radio networks (5G): progress taxonomy and open challenges, *J. Netw. Comput. Appl* 168 (2020), 102760.
- [61] A.O. Laiyemo, P. Luoto, P. Pirinen, M. Latva-Aho, Feasibility Studies on the Use of Higher Frequency Bands and Beamforming Selection Scheme for High Speed Train Communication, *Wirel. Commun. Mob. Comput.* vol. 2017 (2017) 1–14.
- [62] M. Hanaoui, M. Rifi, Elliptical slot rectangular patch antenna array with dual band behaviour for future 5G wireless communication networks, *Prog. Electromagn. Res.* vol. 89 (2019) 133–147.
- [63] Solahuddin Bin Azuwa. (2017). The Effect of Shredded Paper as Partial Sand Replacement on Properties of Cement Sand Brick. Bachelor's Degree Thesis, Universiti Malaysia Pahang, Malaysia.
- [64] B.A. Solahuddin, F.M. Yahaya, Effect of shredded waste paper on properties of concrete, *IOP Conf. Ser. Mater. Sci. Eng.* 1092 (1) (2021), 012063, <https://doi.org/10.1088/1757-899x/1092/1/012063>.
- [65] B.A. Solahuddin, F.M. Yahaya, Load-strain behaviour of shredded waste paper reinforced concrete beam, *IOP Conf. Ser. Mater. Sci. Eng.* 1092 (1) (2021), 012063, <https://doi.org/10.1088/1757-899x/1092/1/012063>.
- [66] B.A. Solahuddin, F.M. Yahaya, A review paper on the effect of waste paper on mechanical properties of concrete, *IOP Conf. Ser. Mater. Sci. Eng.* 1092 (1) (2021), 012063, <https://doi.org/10.1088/1757-899x/1092/1/012063>.
- [67] B.A. Solahuddin, F.M. Yahaya, Structural behaviour of shredded waste paper reinforced concrete beam, *Int. J. Adv. Res. Eng. Innov.* 3 (1) (2021) 74–87. (<http://myjms.mohe.gov.my/index.php/ijarei/article/view/12968>).
- [68] B.A. Solahuddin, F.M. Yahaya, Inclusion of waste paper on concrete properties: a review, *Civ. Eng. J. -Tehran* 7 (2021) 94–113, <https://doi.org/10.28991/CEJ-SP2021-07-07>. Special Issue-Innovative Strategies in Civil Engineering Grand Challenges.
- [69] B.A. Solahuddin, A critical review on experimental investigation and finite element analysis on structural performance of kenaf fibre reinforced concrete, *Structures* 35 (November 2021) (2022) 1030–1061, <https://doi.org/10.1016/j.istruc.2021.11.056>.
- [70] B.A. Solahuddin, F.M. Yahaya, Properties of concrete containing shredded waste paper as an additive, *Mater. Today. Proc.* 51 (2022) 1350–1354, <https://doi.org/10.1016/j.matpr.2021.11.390>.
- [71] B.A. Solahuddin, A review on structural performance of bamboo reinforced concrete, *Mater. Sci. Forum* (2022) 75–80, <https://doi.org/10.4028/p-dx1x87.1056MSF>.
- [72] B.A. Solahuddin, Strengthening of reinforced concrete with steel fibre: a review, *Mater. Sci. Forum* 1056 (2017) (2022) 81–86, <https://doi.org/10.4028/p-3g0h57>.
- [73] Solahuddin, B.A. (2022). A Review on The Effect of Reinforcement on Reinforced Concrete Beam-Column Joint Behavior. Proceedings of Malaysian Technical Universities Conference on Engineering and Technology (MUCET) 2021. (<https://crim.utm.edu.my/wp-content/uploads/2022/09/103-209-2101.pdf>).
- [74] Solahuddin, B.A. (2022). Seismic Performance of Reinforced Concrete Beam-Column Joint: A Review. Proceedings of Malaysian Technical Universities Conference on Engineering and Technology (MUCET) 2021. (<https://crim.utm.edu.my/wp-content/uploads/2022/09/104-211-2121.pdf>).



- [75] B.A. Solahuddin, A comprehensive review on waste paper concrete, *Results Eng.* 16 (October) (2022), 100740, <https://doi.org/10.1016/j.rineng.2022.100740>.
- [76] B.A. Solahuddin, F.M. Yahaya, A state-of-the-art review on experimental investigation and finite element analysis on structural behaviour of fibre reinforced polymer reinforced concrete beams, *Heliyon* 9 (3) (2023), e14225, <https://doi.org/10.1016/j.heliyon.2023.e14225>.
- [77] B.A. Solahuddin, F.M. Yahaya, A narrative review on strengthening of reinforced concrete beams using carbon fibre reinforced polymer composite material through experimental investigation and numerical modelling, *Structures* 52 (January) (2023) 666–710, <https://doi.org/10.1016/j.istruc.2023.03.168>.
- [78] B.A. Solahuddin, F.M. Yahaya, Properties of concrete and structural behaviour of reinforced concrete beam containing shredded waste paper as an additive, *Int J. Concr. Struct. Mater.* 17 (2023), 26, <https://doi.org/10.1186/s40069-023-00588-2>.